

Continuum simulation of granular flow in a rotating cylinder

Suchintika Chanda¹, Soniya Kumawat¹, Abhishek Tiwari¹, Rajesh Ranjan², and Anurag Tripathi^{1,*}

¹Department of Chemical Engineering, IIT Kanpur, U.P. 208016, India

²Department of Aerospace Engineering, IIT Kanpur, U.P. 208016, India

Abstract. We perform continuum simulations of the flow behavior of granular materials in a rotating drum. We extend the interFoam solver used for two-phase fluid simulations in open-source CFD software OpenFOAM for simulating dense granular flow in presence of air. The numerical framework involves solving the continuity equation and momentum balance equations for the granular phase as well as the air phase. The interFoam solver utilizes the Volume of Fluid (VOF) method, which is able to track the movement of the interface between the two fluid phases. The granular phase is modeled as a continuum employing the $\mu - I$ rheology proposed by [1] while the fluid phase is simulated as a Newtonian fluid in the laminar regime. We predict the time dependent as well as steady state flow properties such as velocity, inertial number and kinematic viscosity using this model. The two-phase model is able to capture the behavior of various flow regimes observed in a rotating cylinder such as rolling, cascading, cataracting, and centrifuging as reported in literature. In addition, the effect of cylinder aspect ratio and the influence of the fill fraction of granular material is also accurately captured in these continuum simulations.

1 Introduction

Granular materials are commonly involved in geophysical flows and are widely used in many industries as well. Discrete Element Method (DEM) simulations are commonly employed to simulate the granular flow behavior. Due to the enormous computational cost of large scale DEM simulations, accurate and efficient continuum simulation of granular materials are highly desirable. The modeling of granular material using continuum approach is challenging because of the complex rheology of granular flows ([1, 2]). In recent years, there has been notable progress in investigating the continuum models to predict the flow dynamics of dense granular flow. Two-dimensional collapse of dry granular material was successfully modeled by incorporating the $\mu(I)$ rheology into a finite-volume solver [3]. The authors employed $\mu(I)$ rheology proposed by [1] and successfully predicted the qualitative behavior by comparing it with experimental data. Continuum model by implementing the $\mu(I)$ rheology to predict the steady state properties of flow of granular materials on a heap and flow around a cylinder has also been developed [4]. In addition, [5] used the Mohr-Coulomb elastoplastic (MCEP) model in an eulerian finite element method to simulate granular flow in a rotating drum. They also reported the qualitative comparison of model predictions with experiments.

Furthermore, [6] developed continuum approach to study two-dimensional rapid chute flows of granular materials with a pressure-dependent dynamic slip velocity with a constant friction coefficient assumption. Ref [7]

presented a two-phase flow solver within OpenFOAM for sediment transport applications by employing the $\mu - I$ rheology model. The implemented model is validated with the analytical solution for the laminar bed-load problems. Recent studies (see [8–11]) implemented the $\mu(I)$ rheology in OpenFOAM and were able to predict the qualitative behavior in different flow geometries. Following a similar approach, we present a continuum model for predicting the different flow properties of granular materials in free surface flows, focusing on the case of rotating cylinder in this work. The model captures the evolution of flow properties in rolling as well as cascading regime well and is able to capture the effect of cylinder aspect ratio on free surface profile correctly.

2 Continuum model

We consider a free surface flow of granular materials in a rotating drum composed of identical spherical particles with diameter d and density ρ_p . In the continuum model, a two-phase system is considered, with granular materials being the first phase and air as the second phase. Both fluid phases are assumed to be incompressible. We use the volume of fluid (VOF) approach to model the interface between the two fluid phases, considering the mixture as a single fluid. Hence, the mass and momentum balance equations are given as follows:

$$\nabla \cdot \vec{u} = 0, \quad (1)$$

$$\rho \left(\frac{\partial \vec{u}}{\partial t} + \nabla \cdot (\vec{u} \vec{u}) \right) = \nabla \cdot \underline{\underline{\tau}} - \nabla P + \rho \vec{g}, \quad (2)$$

*e-mail: anuragt@iitk.ac.in

where, \vec{u} , ρ , and $\underline{\underline{\tau}}$ represent the volume weighted average velocity, mixture density and deviatoric phase stress tensor respectively. The volume weighted average of the physical properties is calculated as $\vec{u} = \sum_k \alpha_k \vec{u}_k$, $\rho = \sum_k \alpha_k \rho_k$, $\underline{\underline{\tau}} = \sum_k \alpha_k \underline{\underline{\tau}}_k$, where α_k represents the volume fraction of the k^{th} fluid phase. The deviatoric phase stress tensor ($\underline{\underline{\tau}}_k$) of k^{th} phase is given as $\underline{\underline{\tau}}_k = \eta_k \underline{\underline{\dot{\gamma}}}$, where η_k is viscosity of k^{th} phase. The strain rate tensor $\underline{\underline{\dot{\gamma}}}$ is calculated as $\underline{\underline{\dot{\gamma}}} = (\nabla \vec{u}) + (\nabla \vec{u})^T$. P and \vec{g} are the pressure and gravitational acceleration, respectively.

The VOF equation for phase fraction of k^{th} phase (α_k) is expressed as:

$$\frac{\partial \alpha_k}{\partial t} + \nabla \cdot (\alpha_k \vec{u}) + \nabla \cdot (\vec{u}_r \alpha_k (1 - \alpha_k)) = 0. \quad (3)$$

Here, \vec{u}_r represents the relative velocity between the phases, and we utilize the same approach as in [9] to calculate the \vec{u}_r . The third term in the VOF equation 3 acts only at the interface (where $0 < \alpha < 1$), ensuring a sharp interface by compressing it, with $\alpha = 0.5$ representing the interface boundary.

In order to calculate the effective viscosity of the grain phase, we use the $\mu - I$ rheological expressions [1, 2] for dense flows. In the case of granular materials, the shear stress τ is related to the pressure P through the effective friction coefficient $\mu(I)$, expressed as $\tau = \mu(I)P$. Hence, the effective viscosity for grain phase is given as

$$\eta = \frac{\mu(I)P}{\|\dot{\gamma}\|}, \quad (4)$$

where $\|\dot{\gamma}\|$ is the second invariant of strain-rate tensor, defined as $\|\dot{\gamma}\| = \sqrt{\frac{1}{2}tr(\underline{\underline{\dot{\gamma}}})}$. The empirical correlation of effective friction coefficient $\mu(I)$ using JFP model [1] is given as

$$\mu(I) = \mu_s + \frac{\mu_m - \mu_s}{1 + I_o/I}. \quad (5)$$

The dimensionless inertial number is expressed as $I = \frac{d\|\dot{\gamma}\|}{\sqrt{P/\rho_p}}$ and μ_s, μ_m, I_o are material-dependent rheological parameters. The parameters for the granular phase used in this study are taken from [8] and are listed in Table 1.

Table 1. Parameters of the implemented viscosity model

μ_s	μ_m	I_o	v_{max} (m ² /s)	ρ_p (kg/m ³)	ϕ	d (m)
0.39	0.55	0.279	500	2460	0.6	0.00109

Furthermore, we solve the coupled system of mass (eq. 1) and momentum (eq. 2) equations along with the $\mu(I)$ rheology to obtain the velocity and pressure fields in the open-source software OpenFOAM. We use the interFoam solver for two-phase fluid flow, incorporating the incompressible $\mu(I)$ rheology into the viscosity model. The air phase is modeled as a Newtonian fluid with a constant viscosity and density. For the granular phase, the kinematic viscosity $\nu = \frac{\eta(P,I)}{\rho_b}$, where $\rho_b = \phi \rho_p$ represents the bulk density of the granular phase, with ϕ denoting the volume

fraction of the grains.

$$\nu = \min \left(\frac{\mu(I)P}{\phi \rho_p \|\dot{\gamma}\|}, \nu_{max} \right) \quad (6)$$

We assume a constant packing fraction of $\phi = 0.6$, treating the granular phase as an incompressible fluid. As $\dot{\gamma}$ increases, the viscosity remains finite and is directly proportional to both $\mu(I)$ and P . However, for very low values of $\dot{\gamma}$, the kinematic viscosity ν is numerically bounded by introducing a maximum viscosity, ν_{max} i.e., (eq. 6). The value of ν_{max} is chosen to be $10^2 - 10^4$ times the minimum value of ν [12]. Using the model, we simulate flow of granular and air phase in a rotating cylinder with a diameter of $200d$ and width $40d$, where d is the diameter of the particles comprising the granular phase. We perform simulations with adaptive mesh size on an average grid size of $0.35d$ with a maximum time step of $10^{-4}s$. We impose no-slip boundary condition for the velocity field on all walls and neumann boundary conditions for the pressure field and volume fraction α .

3 Results and discussion

In this section, we report the continuum model predictions for dry monodisperse granular materials flowing in a three dimensional (3D) rotating cylinder. A grid dependency test has been performed, with mesh sizes ranging from coarser to finer grids, to ensure that the simulated flow properties do not change significantly by the varying grid sizes. Figure 1 shows the different flow regimes for

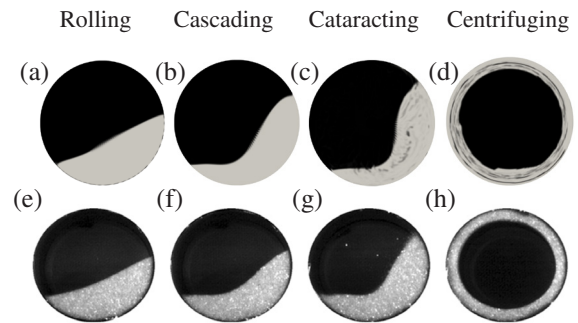


Figure 1. Steady state snapshots of different flow regimes for 30% fill fraction ($f = 0.3$) of granular materials flowing in a rotating cylinder (radius = 0.1m) using the continuum model in different flow regimes. Light gray color represents the grain phase ($\alpha_{grain} = 1$) and black color represents the air phase ($\alpha_{grain} = 0$). The experimental results of [13] corresponding to these flow regimes as are shown in (e) - (h), respectively for qualitative comparison.

granular mixture flowing in a rotating cylinder at different rotational velocities. The filling fraction of grains is $f = 0.3$. The light gray color represents the grain phase ($\alpha_{grain} = 1$) while the black color represents the air phase ($\alpha_{grain} = 0$). Figures 1a, 1b, 1c, and 1d show the results for $\omega = 0.3, 4.05, 8.81$ and 37.06 rad/s, respectively. For $\omega = 0.3$ rad/s ($Fr = 9.1 \times 10^{-4}$), figure 1a shows that there is uniform, steady flow of particle layer on the

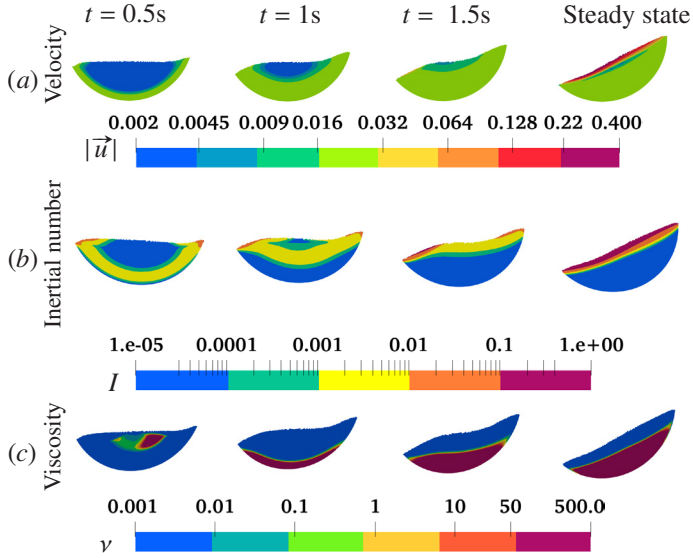


Figure 2. Color maps of different flow properties in the granular phase for 25% fill ratio of grains in the case of rolling regime at different times $t = 0.5s, 1s, 1.5s$ and at steady state (from left column to right): (a) magnitude of velocity $|\vec{u}|$ (m/s), (b) inertial number (I) and (c) kinematic viscosity ν (m^2/s).

surface while most of the particle bed is transported upwards by solid body rotation. Notably, the bed surface exhibits a constant slope surface for the rolling regime at low rotational velocities. Continuum model prediction for α qualitatively matches with the experimental observations of [13] at the same Fr number, as shown in figure 1e. For $\omega = 4.05 \text{ rad/s}$, the interface results in the characteristic S-shaped profile of the cascading regime, shown in figure 1b. The figure 1c shows that for $\omega = 8.81 \text{ rad/s}$, the grain-air interface is no longer smooth and shows air pockets being trapped in the cataracting regime. This observation has been reported by [8] as well. For high value of $\omega = 37.06 \text{ rad/s}$ the Froude number exceeds unity ($Fr > 1$), the flow transitions to the centrifuging regime (figure 1d). Thus, we find that our continuum model is qualitatively able to capture all the four different regimes such as rolling, cascading, cataracting and centrifuging in the rotating cylinder, and show good qualitative agreement with the experimental observations of [13] (second row of figure 1). Quantitative comparison is not expected due to the differences in the $\mu - I$ parameters. Next, we report the time evolution of flow properties of interest such as velocity, inertial number and viscosity etc.

Figure 2 shows color maps of various flow properties for a 30% fill fraction in the rolling regime with $\omega = 0.3 \text{ rad/s}$ at different times (time increasing from left to right). Each row represents a different flow property, while each column corresponds to a different time. Figure 2a (first row) corresponds to the color map of the velocity magnitude ($|\vec{u}|$) at times $t = 0.5s$ (1st column), $1s$ (2nd column), $1.5s$ (3rd column), and at steady state (4th column). The velocity of the grain phase on the wall equals $R\omega$ and has relatively low magnitude in the centre. It becomes maximum near the interface (or the free surface) at steady state and exhibits solid body rotation. The qualitative behavior of velocity field is similar to the contin-

uum model predictions of [14]. Figures 2b (2nd row) and 2c (3rd row) present color maps of dimensionless inertial number (I) and kinematic viscosity (ν) respectively. Figure 2b shows that the inertial number (hence shear rate) is higher (yellow region) due to the cylinder walls at $t = 0.5s$. This high shear region moves towards the free surface with time and the inertial number becomes maximum at the free surface at steady state. The blue region near the walls corresponds to extremely low I values indicating practically no shear in these regions. The corresponding regions in figure 2a, however, do show a finite velocity magnitude to be present due to the rigid-body-like rotation of granular material in these regions. At steady state, the shearing zone near the free surface depicts $I \in [0.1 - 1]$ while the blue colored region $I \in [10^{-5} - 10^{-4}]$ corresponds to the passive, non-shearing region undergoing pure rotation. Figure 2c shows that the passive region have nearly four orders of magnitude higher values of kinematic viscosity compared to the free surface region. This sharp variation of viscosity over a very small distance is crucial for accurate capturing of the two zones and is possible in our model. Note that the maximum viscosity value, ν_{max} , occurs in the passive region of the granular phase, resulting from the rigid body rotation of the material with the cylinder.

Next, we report the model predictions for a fill ratio of $f = 0.5$ for rolling and cascading regimes. Figures 3a and 3b show magnitude of velocity field and inertial number of grain phase at the steady state in a rotating cylinder for rolling regime ($\omega = 0.3 \text{ rad/s}$). It is evident that the shapes of the interface (free surface) are nearly flat in the rolling regime. Figures 3c and 3d show the same for cascading regime ($\omega = 4.05 \text{ rad/s}$), where the free surface is found to be S-shaped. The thickness of the shear layer as well as the inertial number and velocities on this layer are found to be higher than the rolling regime.

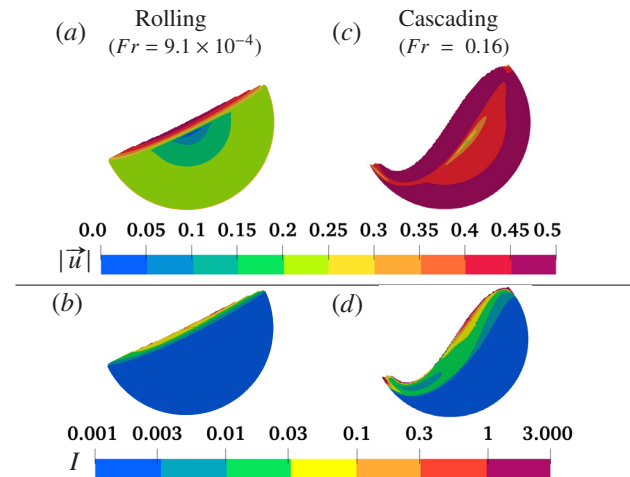


Figure 3. Steady state color maps of granular phase (fill ratio 0.5) for (a) velocity magnitude ($|\vec{u}|$) and (b) inertial number (I) for rolling regime. (c) and (d) show the same for the cascading regime.

Next, we report the effect of aspect ratio of the rotating cylinder, defined as the ratio of the cylinder length to its diameter ($AR = L/D$). Figure 4a shows the predictions of the free surface profiles for two different aspect

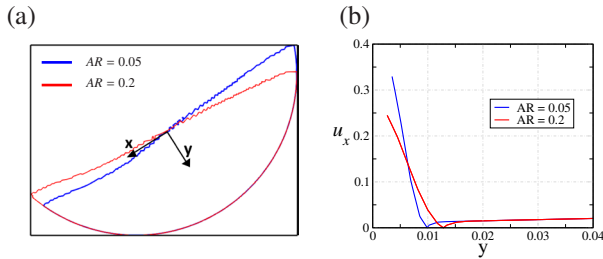


Figure 4. Comparison of (a) free surface profiles and (b) velocity field u_x along y -direction for two different aspect ratios of rotating cylinder with $AR = 0.05$ (blue), and $AR = 0.2$ (red) for $f = 0.25$ and rotational speed $\omega = 0.3 \text{ rad/s}$ in rolling regime.

ratios $AR = 0.05$ (blue), and $AR = 0.2$ (red). Figure 4b shows that the higher inclination angle of the free surface leads to higher free surface velocity for low aspect ratio case. Evidently, the model is able to capture the experimental and simulation observation that the dynamic angle of repose increases with decrease in aspect ratio due to the increased influence of the walls.

4 Summary

In this work, we have studied the flow behavior of dry monodisperse granular materials flowing in the rotating cylinder. We solved the coupled system of mass and momentum balance equations for the two-phase flow by incorporating the $\mu(I)$ rheological model [1] for the grain phase into interFOAM solver of an open-source CFD software OpenFOAM. Unlike previous studies ([15]), we incorporated a varying pressure field into the viscosity model instead of assuming a constant pressure. Our continuum model effectively captures the sequence of rolling, cascading, cataracting, and centrifuging flow regimes classified by [8] based on the Froude number (Fr) range. In addition, the model is able to predict the qualitative behavior of different flow properties such as velocity, inertial number and kinematic viscosity in the different flow regimes at transient as well as steady state, providing insights into the dynamic behavior of granular materials. We have investigated the effect of cylinder aspect ratio analyzing their influence on the granular flow behavior. We shall employ the implemented $\mu(I)$ model to study granular flow behavior in more complex geometries such as hoppers and other industrial equipment.

Acknowledgements

The support and resources provided by PARAM Sanganak under the National Supercomputing Mission, Government of India at the IIT Kanpur are gratefully acknowledged.

References

[1] Jop, P., Forterre, Y., and Pouliquen, O., A constitutive law for dense granular flows. *Nature* **441**, 727–730 (2006).

[2] Forterre, Y., and Pouliquen, O., Flows of dense granular media. *Annu. Rev. Fluid Mech.* **40**, 1-24, (2008).

[3] Lagrée, P.-Y., Staron, L., and Popinet, S., The granular column collapse as a continuum: validity of a two-dimensional Navier-Stokes model with a $\mu(I)$ - rheology. *Journal of Fluid Mechanics* **686**, 378-408 (2011).

[4] Chauchat, J., and Médale, M., A three-dimensional numerical model for dense granular flows based on the $\mu(I)$ rheology. *Journal of Computational Physics* **256**, 696-712 (2014).

[5] Zheng, Q., and Yu, A.B., Modelling the granular flow in a rotating drum by the Eulerian finite element method. *Powder technology* **286**, 361–370 (2015).

[6] Domnik, B., and Pudasaini, S.P., Full two-dimensional rapid chute flows of simple viscoplastic granular materials with a pressure-dependent dynamic slip-velocity and their numerical simulations. *Journal of Non-Newtonian Fluid Mechanics* **173**, 72-86 (2012).

[7] Chauchat, J., Cheng, Z., Nagel, T., Bonamy, C., and Hsu, T.-J., SedFoam-2.0: a 3D two-phase flow numerical model for sediment transport. *Geoscientific Model Development*. **10**, 4367-4392 (2017).

[8] Arseni, A., De Monaco, G., Greco, F., and Maffettone, P.L., Granular flow in rotating drums through simulations adopting a continuum constitutive equation. *Physics of Fluids* **32**, (2020).

[9] Barker, T., Rauter, M., Maguire, E.S.F., Johnson, C.G., and Gray, J.M.N.T., Coupling rheology and segregation in granular flows. *Journal of Fluid Mechanics* **909**, A22 (2021).

[10] Rauter, M., The compressible granular collapse in a fluid as a continuum: validity of a Navier–Stokes model with-rheology. *Journal of Fluid Mechanics* **915**, A87 (2021).

[11] Maguire, E.S.F., Barker, T., Rauter, M., and Johnson, C.G., and Gray, J.M.N.T., Particle-size segregation patterns in a partially filled triangular rotating drum. *Journal of Fluid Mechanics* **979**, A40 (2024).

[12] Staron, L., Lagrée, P.-Y., and Popinet, S., Continuum simulation of the discharge of the granular silo: a validation test for the $\mu(I)$ visco-plastic flow law. *The European Physical Journal E* **37**, 1-12 (2014).

[13] Santos, D.A., Petri, I.J., Duarte, C.R., and Barrozo, M.A.S., Experimental and CFD study of the hydrodynamic behavior in a rotating drum. *Powder technology* **250**, 52-62 (2013).

[14] Qi, H., Xu, J., Zhou, G., Chen, F., Ge, W., and Li, J., Numerical investigation of granular flow similarity in rotating drums. *Particuology* **22**, 119–127 (2015).

[15] Mandal, S., Turek, S., Schwarze, R., Hausteiner, M., Ouazzi, A., and Gladky, A., Numerical benchmarking of granular flow with shear dependent incompressible flow models. *Journal of Non-Newtonian Fluid Mechanics* **262**, 92-106 (2018).